

Finite Size Polyelectrolyte Bundles at Thermodynamic Equilibrium

Mehmet Sayar^{*†} and Christian Holm^{†‡}^{*} Koc University, College of Engineering, Istanbul, Turkey[†] Max-Planck-Institut für Polymerforschung, Mainz, Germany[‡] FIAS, J.W. Goethe - Universität, Frankfurt, Germany

April 14, 2018

Abstract

We present the results of extensive computer simulations performed on solutions of monodisperse charged rod-like polyelectrolytes in the presence of trivalent counterions. To overcome energy barriers we used a combination of parallel tempering and hybrid Monte Carlo techniques. Our results show that for small values of the electrostatic interaction the solution mostly consists of dispersed single rods. The potential of mean force between the polyelectrolyte monomers yields an attractive interaction at short distances. For a range of larger values of the Bjerrum length, we find finite size polyelectrolyte bundles at thermodynamic equilibrium. Further increase of the Bjerrum length eventually leads to phase separation and precipitation. We discuss the origin of the observed thermodynamic stability of the finite size aggregates.

1 Introduction:

Aggregation phenomena in charged macromolecular systems are well known and have been the focus of many investigations, see recent theoretical reviews [1, 2, 3, 4]. Here, we are interested in understanding the aggregation behavior of rod-like charged polyelectrolytes, such as DNA [5], F-actin[6, 7], and microtubules[6] that self-organize into bundles under the influence of only electrostatic interactions. Probably the most investigated systems are solutions of DNA in the presence of multivalent counterions (see Refs. in [8]), which form a variety of different morphologies such as single or multiple toroids, or bundle-like aggregates. The origin of the attraction are short range ionic correlations of multivalent counterions, a phenomenon that cannot be explained on the level of mean-field theories like Poisson-Boltzmann [1, 2, 3, 4]. Simulations have already demonstrated this effect a long time ago [9], but with the uprise of biological physics, it has regained interest in recent years. Many theoretical and computational studies have dealt with the origin of the attraction, and we have an excellent qualitative understanding of it (see Refs. in [1, 2, 3, 4]).

In a solution of many macromolecules, where multi-body effects are present, it has been difficult to obtain accurate enough analytical insight into the aggregate size distribution. The aggregate size must be determined by the competition between the surface tension (due to short range attractions), the repulsive self-energy of the backbone charges, and the entropic degrees of freedom of the counterions. These effects are all coupled, and therefore pose a considerable challenge to analytical approaches. For DNA, it has been argued [10, 3, 11, 12] that the observed finite size of the aggregates is a kinetic effect based on the formation of an energy barrier, and not a consequence of equilibrium thermodynamic properties of the system. Experiments performed with viral DNA support this conjecture at least for the investigated systems [13]. However, recently Henle and Pincus [14] argued that, depending on the actual parameters of the system, finite or infinite bundles should be possible in the presence of short-ranged attractions. Treating the system as consisting of sticky charged rods brings up the analogy to the splitting of a Rayleigh charged hydrophobic droplet, where the mean-field model has already been solved by Deserno [15]. He observes that the droplet size is always finite, if the counterions cannot penetrate into the droplet, but that allowing counterion penetration leads either to finite or infinite droplet sizes, depending on the parameters. There have been relatively few simulations on bundle formations, notable exception being the simulations by Stevens [16, 17], showing the possibility that multivalent ions alone can lead to bundle formations, and the work of Borukhov et al. [18], which focuses on two-rod systems bundled via short range mobile linker interactions. In the present work we investigate the bundle formation for a system of monodisperse charged semi-flexible polymers in the presence of trivalent counterions. This system was chosen since it is known to have short range attractions if the electrostatic interactions are sufficiently large. We investigate the aggregate size distribution as a function of interaction strength, and demonstrate clearly the existence of thermodynamically stable finite size aggregates.

Note that there are also synthetic rod-like polyelectrolytes, such as poly(paraphenylene) oligomers [19], that form stable well defined cylindrical micelles due to hydrophobic interaction of their side chains [20, 21]. Even though the dominant cause of attraction is of non-electrostatic origin, their stability diagram has some relation to the DNA-like systems under investigation which is clear if one considers an Ansatz like in Ref. [15].

In the first section we will present the model for our computational approach. In the following results and discussion section we will present the phase diagram for this system, and explain the origin of the stability of the finite size aggregates. We end with our conclusions.

2 Model:

In this study a coarse-grained representation of polyelectrolyte (PE) chains and trivalent counterions is used. All particles interact with purely repulsive Lennard-Jones interactions (Eqn. 1) with cut-off distance $r_{cut}/\sigma = 2^{1/6}$, in-

teraction strength $\epsilon_{LJ} = k_B T$, and the same diameter σ . Each PE chain is composed of 30 negatively charged beads connected with FENE bonds (Eqn. 2) with a spring constant of $k_F = 7k_B T$ and cut-off distance $R_F/\sigma = 2$. The PE chains are semi-flexible with a harmonic bending potential (Eqn. 3) of stiffness $k_\theta = 100k_B T$. We are interested in the dilute regime where the bundle-bundle contacts could be ignored. The PE monomer number density is fixed for all simulations as $\rho/\sigma^{-3} = 7.5 \cdot 10^{-5}$. There are a total number of 61 PE chains and 10 trivalent counterions per chain in the cubic simulation box, where periodic boundary conditions were used. The unscreened coulomb interactions (Eqn. 4) are calculated using a version of the P3M method[22]. In Eqn. 4, λ_B is the Bjerrum length and is used to control the strength of the electrostatic interactions. We used MD simulations with a time step of $\Delta t = 0.005\tau$, where τ is the usual Lennard-Jones time unit, using the Espresso package[23].

$$U_{LJ}(r) = 4\epsilon_{LJ} \left(\left(\frac{\sigma}{r} \right)^{12} - \left(\frac{\sigma}{r} \right)^6 \right) \text{ for } r < r_{cut} \quad (1)$$

$$U_F(r) = \frac{1}{2} k_F R_F^2 \ln \left(1 - \left(\frac{r}{R_F} \right)^2 \right) \text{ for } r < R_F \quad (2)$$

$$U_\theta(r) = \frac{1}{2} k_\theta \theta^2 \quad (3)$$

$$U_C(r_{ij}) = \lambda_B k_B T \frac{q_i q_j}{r_{ij}} \quad (4)$$

The simulation of stiff-chain PEs with trivalent counterions possess a multitude of difficulties because of the long-range electrostatic interactions and energy barriers. In our previous study[20] on bundles of hydrophobically modified PEs, we have shown that one can obtain a phase diagram by studying the stability of different size aggregates as a function of hydrophobic interaction strength and Bjerrum length. In that study, MD simulations with a Langevin thermostat were used to look at the stability of a preformed assembly of the PEs.

Simulations of the current PE system without explicit hydrophobic interactions with the same approach as in Ref. [20] showed that, for low values of the Bjerrum length ($\lambda_B/\sigma \leq 1.70$), bundles are not stable. The initial bundle quickly falls apart. At equilibrium one occasionally observes short-lived dimers and trimers, but bigger aggregates are not observed. On the other hand for $\lambda_B/\sigma \geq 1.80$ the situation changes drastically. If one starts from aggregates up to size $N = 12$ (N is the number of PEs in the bundle), a fraction of PEs split up, but a finite size aggregate remains in solution. The size of the remaining aggregate depends on the size of the starting bundle. However, as the aggregate size is set to $N \geq 19$ the bundles remain stable throughout the simulation. Beyond $\lambda_B/\sigma = 2.0$ independent of the bundle size, no PEs disintegrate from the start-up bundle. The reason for this interesting behavior could be explained by two different scenarios. By looking at this as a nucleation problem one can argue that for $\lambda_B/\sigma = 1.8 - 2.0$ the critical nucleus size is larger than 19 molecules.

Since the bundles we have studied are smaller than the critical nucleus size the bundles never fall apart completely or grow bigger, but one observes large fluctuations in the bundle size. We have tested this by studying an aggregate of size 25 with additional dispersed rods in solution for $\lambda_B/\sigma > 2.0$. After an integration time of $5 \cdot 10^4 \tau$ no aggregate growth is observed, which leads us to conclude that this is not just a nucleation phenomenon.

Another explanation for this behavior could be high energy barriers for the PEs to split up. This led us to believe that the Langevin thermostat is not efficient enough to overcome such energy barriers, which are highly dependent on λ_B and aggregate size. The parallel tempering method (PT) [24, 25] with Bjerrum length as the tempering parameter was chosen to overcome such energy barriers. We have set up 49 ensembles with λ_B/σ ranging from 1.50 – 2.19. For the simulation of the individual ensembles, we have employed a hybrid Monte Carlo method (HMC)[26, 27]. We integrated for 50τ for each HMC trial, which yields a good combination of acceptance ratio and efficient sampling of the configurational space. For each PT exchange attempt, we have done 9 HMC moves, which we call one cycle. The acceptance ratio of the HMC moves largely depends on the aggregate size distribution, and decreases rapidly for large bundle sizes. In order to test the efficiency of the PT+HMC method for the PE chains, we have conducted two separate simulations with 19 molecules each. The starting configurations were chosen as a single bundle for the first simulation and randomly distributed PEs for the second. After both of the PT+HMC simulations are equilibrated, an identical aggregate size distribution is observed. The results presented in the following section are obtained from PT+HMC simulation with 61 PEs and neutralizing trivalent counterions. All ensembles are started from a configuration of randomly distributed rods. The set of ensembles have been equilibrated for up to 3500 cycles, and data is collected from an additional run of at least 2500 cycles, which took roughly three cpu years on Intel Xeon processors (2.4 GHz).

3 Results and Discussion:

We will start our analysis with the aggregate size distribution obtained from the PT+HMC simulation for the range of Bjerrum length values ($\lambda_B/\sigma = 1.50 - 2.19$). In order to define the aggregation state of the system, we assumed that any trivalent counterion closer than 3σ is condensed onto a PE. If two PEs share one or more condensed counterions they are assumed to be part of the same bundle. The number average ($N_n = \sum N_i f_i$) and weighted average ($N_w = \sum N_i^2 f_i / \sum N_i f_i$) aggregate size (where f_i is the fraction of aggregates of size N_i), as well as the polydispersity index (N_w/N_n) is shown in Fig. 1. In the weak electrostatic regime ($\lambda_B/\sigma \rightarrow 0$) one observes only single PEs in solution, and therefore the polydispersity index is exactly one. For low λ_B (up to $\lambda_B/\sigma = 1.80$) mostly single dispersed rods and occasionally short-lived dimers and trimers can be seen in solution, in agreement with our earlier ob-

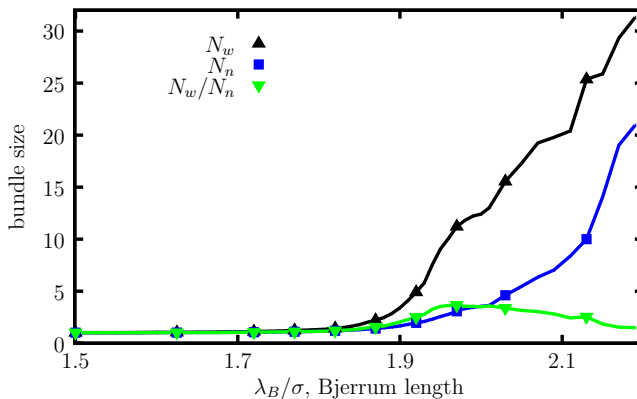


Figure 1: The weighted (N_w) and number average (N_n) bundle size as a function of Bjerrum length (λ_B). For $\lambda_B/\sigma \approx 1.80 - 2.00$ bundles of finite size are observed at thermal equilibrium. The N_w increases with λ_B and the polydispersity index has a maximum at $\lambda_B/\sigma \approx 1.95$.

servations. At such low values of λ_B , even though the net charge of the rods is highly reduced by the condensed counterions, the repulsive interactions among PEs dominate the system behavior, and the polydispersity index is very close to one. Beyond $\lambda_B/\sigma \approx 1.80$ a gradual increase in the average aggregate size is observed. This clearly shows that finite size PE bundles exist at thermodynamic equilibrium for a range of λ_B values. In this range the electrostatic interactions provide both the glue required for aggregation through short range correlations, and also the repulsive forces, which terminate aggregate growth. The entropic penalty still keeps counterions in solution and prevents complete phase separation. Upon aggregation the polydispersity index rises above one, and shows a peak value of 3.7 around $\lambda_B/\sigma = 1.97$. In the high λ_B regime ($\lambda_B/\sigma \geq 2.1$) the correlational attractions dominate, the entropic terms become negligible, and one expects the formation of an infinitely large bundle with a dilute solution of PEs. Therefore the polydispersity index should go to one again, which it does. Since we have only 61 PEs in our simulation box, once the average aggregate size reaches above 20, finite size effects dominate, and one cannot obtain a conclusive answer for the actual average aggregate size.

One can observe the onset of aggregation by looking at the potential of mean force (PMF) among the centers of mass of the rods. However, the PMF of two rods still depends on the relative orientations [11, 28]. Instead, we have chosen to look at the PMF of the PE monomers (Fig. 2), which is obtained by inverting their radial distribution function. We have performed an extra simulation with $\lambda_B/\sigma = 1.0$ to demonstrate the purely repulsive regime. Already for $\lambda_B/\sigma = 1.5$, the effective charge of the PEs is highly reduced and at short distances a weak attractive interaction ($\approx k_B T$) is observed. As seen in Fig. 1 this weak attraction is not sufficient to keep even two PEs together. The presence of

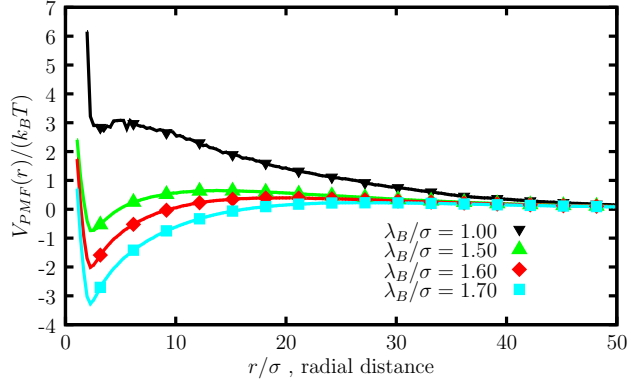


Figure 2: The potential of mean force among PE monomers. The purely repulsive interaction ($\lambda_B/\sigma = 1.0$) is replaced with a weak attraction already for $\lambda_B/\sigma = 1.5$. A small energy barrier is observed at a finite distance. As λ_B is increased further the attraction becomes stronger and the energy barrier disappears, leading to the onset of aggregation into PE bundles.

a weak energy barrier is also observed for $\lambda_B/\sigma = 1.5$. As one increases λ_B further the energy barrier disappears, and the binding energy due to counterion correlations is significantly increased, leading to the formation of stable finite size aggregates.

The distribution of PEs among different size aggregates at fixed λ_B reveals that this is indeed a micellization phenomenon[29] (Fig. 3). For $\lambda_B/\sigma = 1.84$ more than 60% of the PEs exist as dispersed single rods, whereas long-lived dimers and trimers exist in equilibrium with the single PEs. Upon further increase of ($\lambda_B/\sigma = 1.94$) a peak for a finite aggregate size $N \approx 17$ is observed. At $\lambda_B/\sigma = 1.99$ the distribution broadens, and no single distinguishable peak remains.

Next, we will look at the effective line charge density (f_e) of different size bundles. For calculating f_e , we assume that a bundle can be approximated as a rod-like charged object. The net charge of the bundle (PEs and condensed counterions) is divided by the length of the PEs to obtain f_e . Note that these bundles have a finite diameter and small aspect ratio. Furthermore, the PEs are not perfectly aligned, but one observes large fluctuations along the bundle axis. In Fig. 4 we plot f_e for aggregates of size 1, 2, 5, 10, and 23 as a function of λ_B . For single PEs f_e decreases linearly up to $\lambda_B/\sigma \approx 1.8$. Beyond this value we observe a quick convergence of f_e to a plateau value of ≈ 0.1 . If we look at f_e obtained for a single PE simulated at the same density within the cell model, no such convergence is observed. The cell model simulations match with many-rod PT+HMC simulations only for low λ_B . This mismatch demonstrates the importance of many body effects, such as aggregation of PEs into bundles. For the many-rod simulation we see that beyond $\lambda_B/\sigma > 1.8$ most of the single PEs

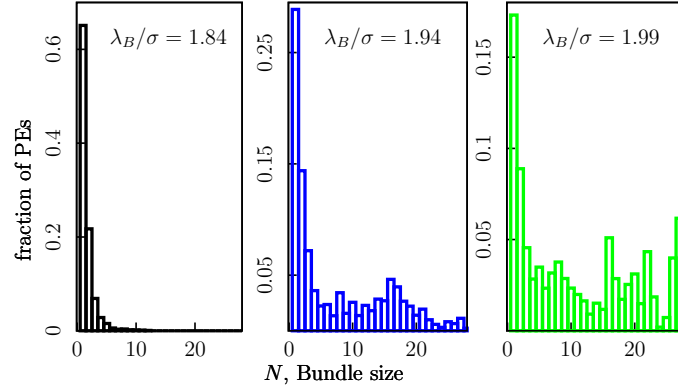


Figure 3: The distribution of PEs among different size aggregates. Beyond the critical λ_B a micellization type size distribution is observed, where monomers are in equilibrium with finite size PE bundles.

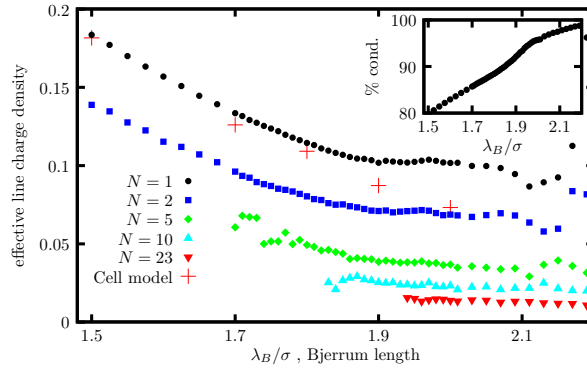


Figure 4: Effective line charge density (f_e) as a function of λ_B for aggregates composed of N rods. At $\lambda_B \approx 1.8\sigma$ the average aggregate size strongly increases, which leads to a flattening of f_e . For comparison we show f_e of a single PE in the cell model, where multi-body effects are not present. In the insert the total fraction of condensed counterions is shown as a function of λ_B .

compensate a high fraction of their intrinsic charge via condensing counterions. As a result the repulsion among PEs is greatly diminished and the single PEs with the lowest line charge density aggregate to form bundles, leaving behind only the single PEs with higher f_e . Upon aggregation of PEs, the trivalent counterions gain enthalpy, without diminishing the system entropy further more. Therefore f_e for single PEs deviates from the cell model. For aggregates of size of 2, 5, 10, and 23 a similar behavior is observed. The reduction in f_e continues until merging into even bigger aggregates becomes feasible, lowering the free energy even more. Note that large aggregate sizes are only observed beyond a certain λ_B value. For example, for $N = 5$ the high fluctuations in f_e around $\lambda_B/\sigma \approx 1.7$ stem from the fact that these aggregates are very rare at such λ_B values. The insert in Fig. 4 denotes the total fraction of condensed counterions over all PEs. This fraction increases linearly up to $\lambda_B/\sigma \approx 1.8$. Beyond $\lambda_B/\sigma \approx 2.0$ the charge compensation begins to saturate. Note that at this point more than 95% of the charge on the PEs are compensated, and only a small fraction of counterions are left in solution. Therefore the entropic penalty associated with condensing these remaining free counterions is extremely high. The deviation from the linear regime nicely coincides with the onset of aggregation.

If we want to map our results to biomolecules such as DNA in a trivalent counterion solution we can do so by requiring that the strong coupling parameter Ξ [4] for this system is the same ($\Xi \approx 80$). For our model this is achieved for $\lambda_B \approx 1.3$, where we do not yet observe aggregation. This is due to the short length of our rods. For short rods counterion condensation is much weaker [30] due to end effects, and therefore one needs stronger electrostatic interactions to observe attraction and bundle formation.

4 Conclusions:

We investigated the aggregation behavior of semi-flexible polyelectrolytes with trivalent counterions. In dilute solutions the system shows a micellization type aggregate size distribution. At low values of the Bjerrum length single dispersed PEs are found, whereas at the other extreme of large couplings macroscopic phase separation is observed. Our most important finding is that finite size aggregates exist at thermodynamic equilibrium for a small window of Bjerrum length values. The aggregate size distribution of these PE bundles is rather broad. The finite size aggregates are a result of the correlation of the trivalent counterions at short distances, and repulsive electrostatic interactions at long distances. The entropic terms due to counterions, and end-effects due to the finite length of the PE chains also contribute to this delicate balance. The fraction of condensed counterions are found to be significantly lower than those for an infinite PE rod, which leads to an increased counterion entropy.

5 Acknowledgements

We would like to thank the EC for providing a Marie Curie Intra-European Postdoctoral Fellowship to M. Sayar (MCIEF 500604). Additional funding from the DFG through grant SFB 625 and Ho1108/11-3 is gratefully acknowledged. We thank M. Deserno and K. Kremer for stimulating scientific discussions.

References

- [1] Electrostatic Effects in Soft Matter and Biophysics, Vol. 46 of NATO Science Series II - Mathematics, Physics and Chemistry, edited by C. Holm, P. Kékicheff, and R. Podgornik (Kluwer Academic Publishers, Dordrecht, NL, 2001).
- [2] A. Y. Grosberg, T. T. Nguyen, and B. I. Shklovskii, *Rev. Mod. Phys.* **74**, 329 (2002).
- [3] Y. Levin, *Rep. Prog. Phys.* **65**, 1577 (2002).
- [4] H. Boroudjerdi *et al.*, *Physics Reports* **416**, 129 (2005).
- [5] V. Bloomfield, *Biopolymers* **31**, 1471 (1991).
- [6] J. X. Tang, S. Wong, P. T. Tran, and P. Janmey, *Ber. Bunsenges. Phys. Chem.* **100**, 796 (1996).
- [7] J. Käs *et al.*, *Biophysical Journal* **70**, 609 (1996).
- [8] V. A. Bloomfield, *Current Opin. Struct. Biol.* **6**, 334 (1996).
- [9] L. Guldbrand, L. G. Nilsson, and L. Nordenskiöld, *J. Chem. Phys.* **85**, 6686 (1986).
- [10] B.-Y. Ha and A. J. Liu, *Phys. Rev. Lett.* **81**, 1011 (1998).
- [11] B.-Y. Ha and A. Liu, *Europhys. Lett.* **46**, 624 (1999).
- [12] J. F. Stilck, Y. Levin, and J. J. Arenzon, *J. Stat. Phys.* **106**, 287 (2002).
- [13] O. Lambert, L. Letellier, W. Gelbart, and J. Rigaud, *Proc. Natl. Acad. Sci. (USA)* **97**, 7248 (2000).
- [14] M. Henle and P. Pincus, *Phys. Rev. E* **71**, 060801 (2005).
- [15] M. Deserno, *Eur. Phys. J. E* **6**, 163 (2001).
- [16] M. J. Stevens, *Phys. Rev. Lett.* **82**, 101 (1999).
- [17] M. J. Stevens, *Biophys. J.* **80**, 130 (2001).
- [18] I. Borukhov *et al.*, *J. Chem. Phys.* **117**, 462 (2002).

- [19] M. Bockstaller *et al.*, *Macromolecules* **33**, 3951 (2000).
- [20] H. J. Limbach, M. Sayar, and C. Holm, *J. Phys.: Condensed Matter* **16**, S2135 (2004).
- [21] H. J. Limbach, C. Holm, and K. Kremer, *Macromolecular Chemistry and Physics* **206**, 77 (2005).
- [22] M. Deserno and C. Holm, *J. Chem. Phys.* **109**, 7678 (1998).
- [23] H.-J. Limbach, A. Arnold, B. A. Mann, and C. Holm, *Comp. Phys. Comm.* **174**, 704 (2006).
- [24] R. H. Swendsen and J. Wang, *Phys. Rev. Lett.* **57**, 2607 (1986).
- [25] D. Frenkel and B. Smit, *Understanding Molecular Simulation*, 2nd ed. (Academic Press, San Diego, 2002).
- [26] S. Duane, A. D. Kennedy, B. J. Pendleton, and D. Roweth, *Phys. Lett. B.* **195**, 216 (1987).
- [27] A. Irback, *J. Chem. Phys.* **101**, 1661 (1994).
- [28] K.-C. Lee *et al.*, *Phys. Rev. Lett.* **93**, 128101 (2004).
- [29] C. Huang, M. de la Cruz, M. Delsanti, and P. Guenoun, *Macromolecules* **30**, 8019 (1997).
- [30] D. Antypov and C. Holm, *Phys. Rev. Lett.* **96**, 088302 (2006).